Simulation of Pipeline Transport of Carbon Dioxide with Impurities

Mehrnaz Anvari
Fraunhofer Institute for Algorithms and Scientific Computing
Sankt Augustin, Germany
email: Mehrnaz.Anvari@scai.fraunhofer.de

Anton Baldin
PLEdoc GmbH and Fraunhofer Institute for Algorithms and Scientific Computing
Sankt Augustin, Germany
email: Anton.Baldin@scai.fraunhofer.de

Tanja Clees
University of Applied Sciences Bonn-Rhein-Sieg and Fraunhofer Institute for Algorithms and Scientific Computing
Sankt Augustin, Germany
email: Tanja.Clees@scai.fraunhofer.de

Bernhard Klaassen
Fraunhofer Institute for Algorithms and Scientific Computing
Sankt Augustin, Germany
email: Bernhard.Klaassen@scai.fraunhofer.de

Igor Nikitin
Fraunhofer Institute for Algorithms and Scientific Computing
Sankt Augustin, Germany
email: Igor.Nikitin@scai.fraunhofer.de

Lialia Nikitina
Fraunhofer Institute for Algorithms and Scientific Computing
Sankt Augustin, Germany
email: Lialia.Nikitina@scai.fraunhofer.de

Sabine Pott
Fraunhofer Institute for Algorithms and Scientific Computing
Sankt Augustin, Germany
email: Sabine.Pott@scai.fraunhofer.de

***Abstract*—The transport of carbon dioxide through pipelines is one of the important components of Carbon dioxide Capture and Storage (CCS) systems that are currently being developed. If high flow rates are desired, a transportation in the liquid or supercritical phase is to be preferred. For technical reasons, the transport must stay in that phase, without transitioning to the gaseous state. In this paper, a numerical simulation of the stationary process of carbon dioxide transport with impurities and phase transitions is considered. We use the Homogeneous Equilibrium Model (HEM) and the GERG-2008 thermodynamic equation of state to describe the transport parameters. The algorithms used allow to solve scenarios of carbon dioxide transport in the liquid or supercritical phase, with the detection of approaching the phase transition region. Convergence of the solution algorithms is analyzed in connection with fast and abrupt changes of the equation of state and the enthalpy function in the region of phase transitions.**

***Index Terms*—simulation and modeling; mathematical and numerical algorithms and methods; advanced applications; carbon dioxide; capture and storage; pipeline transport.**

I. Introduction

To reduce greenhouse gas emissions into the atmosphere, Carbon dioxide Capture and Storage (CCS) systems are currently being developed. Typically, such systems consist of 3 parts: (1) capturing carbon dioxide (CO_2) at its source; (2) transporting CO_2 through pipelines to special storage sites; (3) and finally injecting it into wells, when underground storage is used. In this paper, we focus on the second part of the aforementioned process. It is generally required that CO_2 be in the liquid or supercritical phase during transport in order to increase the density and mass flows. It is essential to avoid the transition of fluid phase to gas, which leads to cavitation and destruction of the pipeline during transportation. To ensure reliable operation of the CO_2 pipeline, both an extensive experimental base and stable numerical simulation of the transportation process are required. At the same time, for a long-term planning, it is sufficient to simulate a stationary process of the transportation, with CO_2 in a 1-phase state and an indication of a possible phase transition, in order to prevent it.

The pioneering work [1] has considered in detail the stationary process of transporting pure CO_2 through a pipeline and pumping it into an underground storage, taking into account phase transitions. In that and in subsequent papers, the importance of taking into account impurities that have a strong influence on the parameters of the transportation process even at low concentrations, has been pointed out. The papers [2]–[9] considered the process of CO_2 transport, both stationary and dynamic. Papers [1]–[8] consider a Homogeneous Equilibrium Model (HEM), in which different phases of a fluid are homogeneously mixed and have the same speed, pressure, temperature and chemical potential. In papers [4]–[6], [8], [9], phase split is also considered, i.e., when the phases are geometrically separated, and phase slip, i.e., when the phases have different speeds. Also, in works [4], [6], [8] the formation of a solid phase of CO_2 (dry ice) is considered. In the works [5], [6], [8], [9], fast transient processes occurring during depressurization of a pipe are considered, together with the related experiments. The economic aspects of pipeline CO_2

 ISBN: 978-1-68558-073-5

transport have been considered in papers [10]–[13].

In this paper, we describe a stationary simulation of the CO_2 transport process with the possibility of considering impurities, phase transitions, several sources with different composition, and networks of complex topology. Simulations of this type have extended the capabilities of our software MYNTS [14]–[18]. The system provides an open, freely configurable and user-friendly specification of modeling, defined as a list of variables and equations. An open Python code for workflow procedures is also provided. The main calculations are performed in a fast C++ solver. The system also has a Graphical User Interface (GUI) with the ability to edit networks and scenarios. This architecture allows to formulate and quickly solve very large network problems, as well as the ability to model different energy carriers and couple different energy sectors.

For problems of stationary transportation of fluids, we implement standard pipe transport equations with friction terms by Nikuradse [19], Hofer [20] and spatial discretization of type [21]. The GERG equation of state [22], [23], which is currently the ISO standard [24], is used to accurately model the thermodynamics of fluids, in particular CO_2 with impurities and phase transitions. Additionally, we have developed an algorithm for detecting the proximity to the region of phase transitions. A number of numerical experiments were carried out to test the developed algorithms. Based on them, it is shown that the fast, sometimes abrupt, behavior of the system in the presence of phase transitions affects the convergence properties of the numerical algorithms used for the solution. In the scenarios we have considered, the divergence, if it occurs, is entirely localized in the region of phase transitions. On the other hand, scenarios without phase transitions are converging, which makes it possible to solve them with detection of proximity to the region of phase transitions.

Section II reviews the physics of phase transitions applied to CO_2 with impurities. Section III discusses the transport equations used. In Section IV, we describe numerical experiments, with particular attention paid to the questions of convergence of iterative processes. Finally, in Section V, we summarize our results.

II. Physics of phase transitions

Phase transitions occur in slightly different ways for pure substances and their mixtures. Figure 1a shows the phase transition for pure CO_2. At a constant temperature, the pressure decreases starting in the region of the liquid state. There is a line of phase transitions on the diagram. When the pressure decreases, the process proceeds until it intersects with this line, after that the pressure decrease stops until all the fluid passes from the liquid state to the gaseous state. At the same time, Figure 1c shows that during this process, the average density changes from large values, typical for the liquid phase, to small values, typical for a gas. Figure 1b shows what happens in the case of a mixture, here 95% CO_2, 3% N_2, 2% O_2. Now, the 2-phase state corresponds not to a line, but to a region on (T, P)-diagram. The boundary of this region is called the

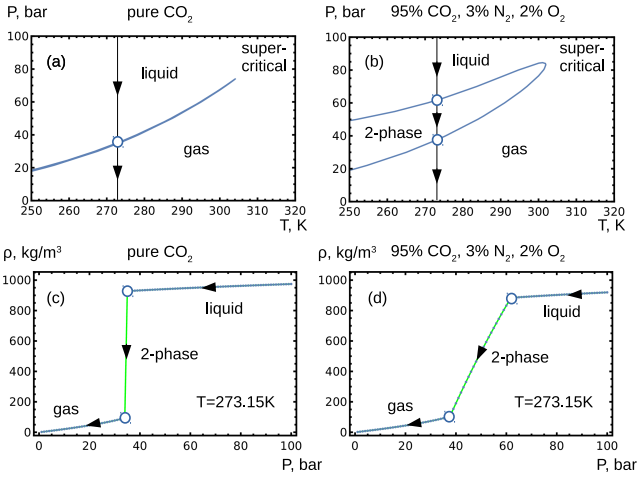

Fig. 1. Phase transitions at fixed temperature: (a),(c) – for pure CO_2; (b),(d) – for CO_2 with impurities.

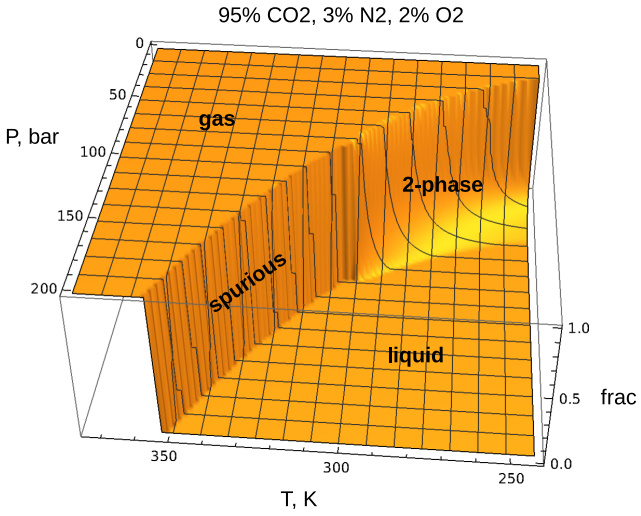

Fig. 2. Fraction of gaseous phase as a function of pressure and temperature.

Vapour-Liquid Equilibrium (VLE) diagram, or *phase envelope*. When the pressure decreases, the point enters this region and the fluid also passes from the liquid state to the gaseous state, but here the pressure continues to decrease. Figure 1d shows that in the 2-phase state, the density decreases in the same way as for pure substance, but at a decreasing pressure.

The 3D diagram in Figure 2 shows the behavior of $frac$-value, which varies in the interval $[0, 1]$ and measures the fraction of the gaseous phase in the fluid. Here, one can also see the region where the phase transition occurs, which proceeds continuously for mixed compositions. Also, this diagram has a jump on a line starting from the critical point, however this transition is spurious. Above the critical point, gas and liquid do not really differ from each other, but according to the scheme of description, it is required to make a transition from gas to liquid somewhere. Although the quantity $frac$ has a formal jump here, the physically measurable quantities have

 ISBN: 978-1-68558-073-5

no jumps on this line.

Interestingly, this surface resembles the surfaces considered in the theory of functions of a complex variable. Namely, if we take this surface, as well as the $1-frac$ surface and join them together, we get an object that looks like a Riemann surface for a complex square root. The similarity is not accidental, in both cases there is a 2-sheeted surface without the possibility of continuously separating the sheets from each other.

For the thermodynamical description of the fluid, the GERG equation of state and its accompanying implementation [22]–[24] is used. Technically, it is delivered as a software library where one can access a variety of functions describing the fluid state. In addition to the already mentioned phase envelope and $frac$-value, we use the Equation Of State (EOS) and energy functions

$$z = z(T, P, x),\ W = W(T, P, x), \tag{1}$$

where T is absolute temperature, P is pressure, x is a vector describing fluid composition, $W = (H, U, G, A)$ is a vector describing molar energies of different types: enthalpy, internal energy, Gibbs energy, Helmholtz energy, respectively. Compressibility factor z enters in the gas law $P = \rho RTz/\mu$, where R is the universal gas constant, ρ is the mass density, μ is the molar mass.

As a parameter important for the user, the $frac$-value or a conservative algorithm based on $frac$-values in the vicinity of the solution can be used to detect the proximity of phase transitions:

Algorithm (proximity-alarm):

```
given (T0,P0,x,dT,dP,val)
for T in (T0-dT,T0,T0+dT)
  for P in (P0-dP,P0,P0+dP)
    if frac(T,P,x)!=val return true
return false.
```

The algorithm considers a 3x3 grid created by $(\pm dP, \pm dT)$-variations, and if $frac$ differs from the user-specified val at least at one point, triggers a proximity alarm. This simple algorithm is applied to every node in the network. It has the advantage that it works even in the networks with many fluid compositions, i.e., variable x-values. Alternative algorithms based on the construction of the phase envelope produce many diagrams for different compositions, which complicates the analysis. At the same time, this algorithm has one drawback, it can produce a false alarm when approaching a spurious line. In this case, the user can visually control the solution trajectory on the (T, P)-diagram by constructing a phase envelope for the local network segment with constant x. The development of other algorithms for automatic detection of phase transitions that work for the variable composition of the fluid in the network is in our future plans.

III. Pipe transport equations

A pressure drop in the pipe in the stationary case is described by the equation:

$$dP/dL = -\lambda\rho v|v|/(2D) - d(\rho v^2)/dL - \rho g\, dh/dL, \tag{2}$$

where L is the running length along the pipe, v is the speed of the fluid, D is the internal diameter of the pipe, g is the gravitational acceleration, and h is the height. On r.h.s. the first term is usually dominant, describing the contribution of the friction force, defined in terms of the dimensionless friction coefficient $\lambda(k/D, Re)$ using the Nikuradse [19] formula or the more accurate Hofer [20] formula. Here, k is the pipe roughness, $Re = 4|Q_m|/(\pi\mu_{visc}D)$ is Reynolds number, where μ_{visc} is the dynamic viscosity and $Q_m = \rho v\pi D^2/4$ is the mass flow constant along the pipe. Further r.h.s. includes the convective and gravitational terms.

For discretization purposes, we consider a short pipe segment of length L and integrate the equation over it. Expressing the velocity in terms of the mass flow, and keeping only the leading first term for illustration, we get $dP/dL = c_1/\rho$, where c_1 is constant. When integrating, we replace the variable density ρ by the average $\bar\rho = (\rho_1 + \rho_2)/2$ over the end points of the segment, i.e., $P_2 - P_1 = c_1 L/\bar\rho$. As an alternative, we multiply the original equation by P, use the gas law $P/\rho = RTz/\mu$, replace the variables T and z with the end averages and, thereby, we get $(P_2^2 - P_1^2)/2 = c_1 LR\bar T\bar z/\mu$, in a more familiar quadratic form for gas dynamics [21]. To find the optimal pipe subdivision, the number of segments is increased until the solution stops changing, up to a given tolerance.

Temperature profiles are described by the equation

$$dH/dL = -\pi D c_h (T - T_s)\mu/Q_m, \tag{3}$$

according to which the enthalpy change in a segment of the pipe is equal to the heat exchange with the soil or other environment. Here, c_h is the heat transfer coefficient, T_s is the soil temperature. Note that when the heat exchange is switched off $c_h = 0$, the process described by this formula is isoenthalpic $dH = 0$, and the temperature change is related to the pressure change by the well-known formula $dT = \mu_{JT} dP$, where $\mu_{JT} = -(\partial H/\partial P)_T/(\partial H/\partial T)_P$ – Joule-Thomson coefficient. The equation can also be modified by introducing kinetic and gravitational terms.

For discretization, in the form $dH/dL = c_2(T - T_s)$ with constant c_2, the variable temperature T is replaced by the constant T_x, which can be taken as the end average $\bar T$ or the value of the outflow temperature T_{out}, which better represents the case of longer segments. After integration, we get $H_2 - H_1 = c_2 L(T_x - T_s)$. Further, in an iterative solution process in which the pressure profile and fluid composition are kept constant, the enthalpy values can be linearized using the formula $H(T^{i+1}) = H(T^i) + c_p(T^i)(T^{i+1} - T^i)$, where the superscripts indicate the number of iterations and $c_p = (\partial H/\partial T)_P$ is the isobaric molar heat capacity, also calculated by the GERG software library.

Next, we will consider in more detail the process of convergence of the iterations used for the solution. In our previous work [18], the architecture of MYNTS system has been described. Due to software-technical reasons, the solution was divided into 2 parts: (1) *Pressure-Massflow (PM)-iterations*,

 ISBN: 978-1-68558-073-5

solved by a sparse non-linear Newtonian solver; and (2) *mix-iterations*, solved by a sparse linear solver. PM iterations determine the pressure, density and mass flow, by solving a relatively small nonlinear system. This system, however, has strong numerical instabilities associated with nearly zero Jacobi matrix eigenvalues and requires special stabilization measures [17]. Mix iterations solve a large linear system defining a multicomponent fluid composition, determine temperature and call external modules, such as GERG that would otherwise be called too often in a fully coupled system. After the temperature linearization described above, all mix equations of the system at each iteration become linear, their solution can be produced by a sparse linear solver such as *Pardiso*. Further, these two processes are iterated, while using an additional stabilization algorithm *weighted relaxation* [18], the result of the combined PM-mix-iteration $h(x)$ is replaced by a weighted average $x_{i+1} = wh(x_i) + (1-w)x_i$.

Among the modeling limitations, it should be mentioned that the GERG module does not consider the solid phase and derives equilibrium conditions for the liquid and gaseous phases under the HEM assumptions. The transport equations considered here treat 2-phase solutions as 1-phase, with the values of thermodynamic parameters calculated by the GERG module in the *total* system, which also means calculations within the HEM framework.

At the end of this section, it is worth to mention a general point regarding the simulation of static and dynamic types. Often, the user assumes the uniqueness of the solutions obtained in the simulations. In general, this may not be the case. Existence and uniqueness theorems for solutions are formulated only in rare cases. So, for example, they are guaranteed for the PM subsystem under the conditions of generalized resistivity [14]. Being combined with the mix system, the uniqueness of the solution is not guaranteed. Theoretically imaginable is the situation when there are two stationary solutions, one 1-phase, the other 2-phase, and it may happen that the stationary solver finds the first one, but in reality the second one will be realized. Consideration of dynamic simulation can decide which solution the trajectory will go to when integrating from a given initial state. But even for a dynamic solver, saddle points, bifurcations of the solution are possible, where, with a small variation, the solution can go in one direction or the other. Questions about the uniqueness of stationary solutions and the stability of dynamic solutions must be investigated in the practical analysis of simulation results.

IV. Numerical experiments

To test the implemented algorithms, we use a pipe segment with parameters taken from [1]. In our experiments, different scenarios are considered, see Table I. In the first scenario, a small flow is set, at which no phase transitions occur. The entire pipe is filled with liquid or supercritical fluid. In the second scenario, a larger flow is set, the pressure drops more strongly, and a phase transition occurs in the system. Both

TABLE I
Parameters of test scenarios

parameter	symbol [units]	value
total pipe length	$L_{tot}[km]$	150
pipe internal diameter	$D[m]$	0.5
pipe roughness	$k[mm]$	0.5
heat transfer coefficient	$c_h[W/(m^2K)]$	4
fluid composition	$x(CO_2, N_2, O_2)$	(0.95,0.03,0.02)
inlet pressure	pset [bar]	100
outlet norm.vol.flow, scen1	qset1 $[10^3 m^3/h]$	200
outlet norm.vol.flow, scen2	qset2 $[10^3 m^3/h]$	310

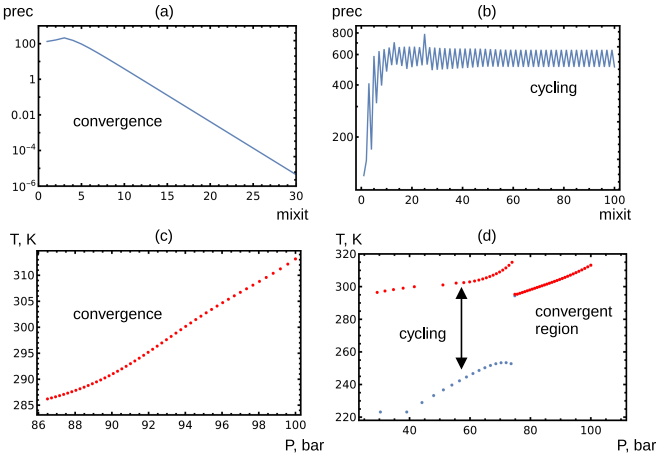

Fig. 3. (a),(c) – convergent iterations for scenario without phase transitions; (b),(d) – cycling iterations for scenario with phase transitions, red color - iteration 100, blue color – iteration 99.

scenarios use a mixture of 95% CO_2, 3% N_2, 2% O_2. The pipe is laid horizontally with $h = 0$.

Figure 3 shows the convergence characteristics for our test scenarios, left column for scen1, right column for scen2. The dimensionless precision parameter $prec = \max(res_i/norm_i)$ is defined as the maximum of the residuals of the equations divided by the normalizing value, for each equation its own. For the Kirchhoff equation of conservation of flow, the friction law in quadratic form, and the gas law expressed with respect to density, the normalization factors $norm = (1kg/s, 100bar^2, 1kg/m^3)$ are chosen, respectively. In our system, the equations and their normalizing factors can be freely configured by the user. For a purely 1-phase solution scen1 shown in Figure 3(a) and (c), the value of $prec$ decreases exponentially with the number of iterations and the solution procedure converges. For scen2, as seen in Figure 1(b) and (d), the procedure has cycling. In more detail, we see that there is a converging region for the 1-phase and a part of the 2-phase state, after which a temperature jump occurs, and oscillations are observed in the remaining pipe segment.

Along with the two main scenarios, we ran a number of additional simulations with small qset variations around the specified values. Simulations show stability of the effects, convergence in the 1-phase solution, and divergence in the 2-phase solution. The reason for this divergence is that EOS

 ISBN: 978-1-68558-073-5

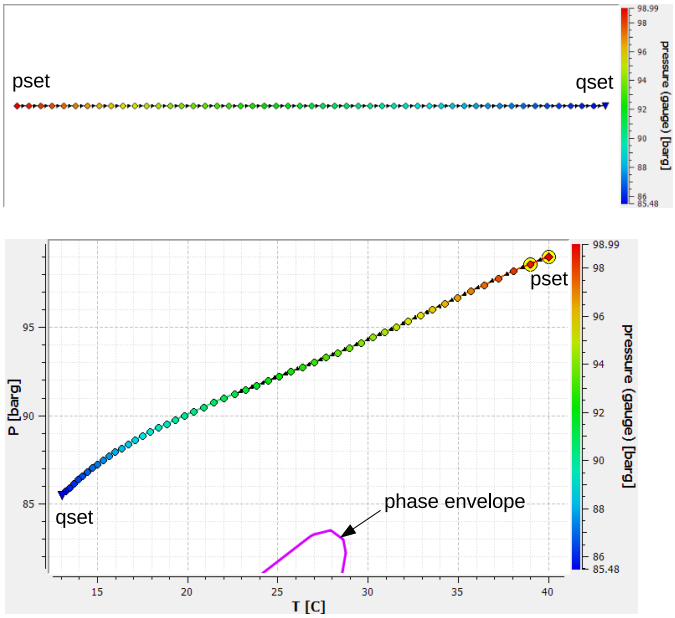

Fig. 4. Screenshot of MYNTS GUI for scenario without phase transitions.

and the enthalpy function receive large derivatives in the phase transition region. These functions are actually jump-like for a pure substance and formally continuous for a mixture, but at a low concentration of impurities, the derivatives are still large.

A prototype example of such instability is the logistic map: $x_{i+1} = rx_i(1-x_i)$, which characterizes the behavior of simple iterations near the root $x = 1-1/r$. When r rises from 1, and passes the value 3, the absolute value of the r.h.s. derivative of the logistic map equation exceeds 1, which is a critical value for the convergence of simple iterations. Below this value, the iterations converge. Above it, limit cycles appear, first with a multiplicity of 2, then they double, and finally the system goes to chaos.

Qualitatively, the same effects happen in our case. The stabilization algorithm used in principle helps to overcome such divergences, but for an ever higher derivative it becomes less and less effective. We are going to explore this problem in more detail in our future work. In order to overcome the divergence, we can try to adjust the weight parameter in the stabilizing algorithm. The dynamic solver behaves in much the same way as weighted relaxation with a low weight; with a decrease in the integration step, the stability of the integration also increases. As shown in Figure 1, high derivatives only occur for EOS in the form $\rho(T, P)$, changing variables to $P(T, \rho)$ could also be a solution of the problem.

At the same time, within the framework of the set technical task, it is required to consider only those scenarios in which there are no phase transitions and also there are no divergences associated with them. For such solutions, it is required to determine the proximity of the solution to the region of phase transitions. That can be done using the proximity-alarm algorithm described above.

Figure 4 shows the screenshots for scen1 solution in MYNTS GUI. At the top, there is the pipe geometry with the pressure profile shown in color. At the bottom, there is the solution on the (T, P)-plane, where a part of the phase envelope is also shown. The yellow disks show the proximity-alarm triggered in the given node for the values $dT = 1K$, $dP = 1bar$. The first 2 nodes near pset appear to be close to the spurious line on the phase diagram. The alarm in them can be canceled, because they are located top-right to the phase envelope, in the supercritical region. In general, this visual criterion is difficult to automate, since phase envelopes can have a more complex appearance than in the figures of this paper. Further, the figure shows how the solution trajectory passes at a safe distance from the phase envelope, providing the required CO_2 transport without phase transitions.

V. Conclusion

In this paper, we have considered a numerical simulation of the stationary process of CO_2 transport with impurities and phase transitions. We have developed the algorithms that allow to solve scenarios of CO_2 transport in the liquid or supercritical phase and to detect the approaching of the phase transition region. We have analyzed a convergence of the solution algorithms in connection with fast and abrupt changes of the equation of state and the enthalpy function in the region of phase transitions.

The performed numerical experiments show that the scenarios with a single CO_2 phase converge. For the obtained temperature and pressure profiles, a conservative algorithm for detecting the proximity of phase transitions can be applied, giving the solution to the technical problem posed. At the same time, divergences can occur in scenarios with phase transitions due to the abrupt change of thermodynamic parameters. Questions about the possible suppression of these divergences as well as improved detection of phase transitions are the subject of our further work.

Acknowledgments

The work has been supported by Fraunhofer research cluster CINES. We acknowledge support from Open Grid Europe GmbH in the development and testing of the software.

References

[1] M. Nimtz, M. Klatt, B. Wiese, M. Kühn, and H.-J. Kraautz, “Modelling of the CO2 process- and transport chain in CCS systems – Examination of transport and storage processes”, Chemie der Erde – Geochemistry, vol. 70, suppl. 3, 2010, pp. 185-192.

[2] S. Liljemark, K. Arvidsson, M. T. P. Mc Cann, H. Tummescheit, and S. Velut, “Dynamic simulation of a carbon dioxide transfer pipeline for analysis of normal operation and failure modes”, Energy Procedia, vol. 4, 2011, pp. 3040-3047.

[3] M. Chaczykowski and A. J. Osiadacz, “Dynamic simulation of pipelines containing dense phase/supercritical CO2-rich mixtures for carbon capture and storage”, International Journal of Greenhouse Gas Control, vol. 9, 2012, pp. 446-456.

[4] P. Aursand, M. Hammer, S. T. Munkejord, and Ø. Wilhelmsen, “Pipeline transport of CO2 mixtures: Models for transient simulation”, International Journal of Greenhouse Gas Control, vol. 15, 2013, pp. 174-185.

[5] L. Raimondi, “CO2 Transportation with Pipelines - Model Analysis for Steady, Dynamic and Relief Simulation”, Chemical Engineering Transactions, vol. 36, 2014, pp. 619-624.

 ISBN: 978-1-68558-073-5

[6] M. Drescher et al., “Towards a Thorough Validation of Simulation Tools for CO2 Pipeline Transport”, Energy Procedia, vol. 114, 2017, pp. 6730-6740.
[7] B. Chen, H. Guo, S. Bai, and S. Cao, “Optimization of process parameters for pipeline CO2 transportation with impurities”, IOP Conf. Series: Earth and Environmental Science, vol. 300, 2019, 022002.
[8] M. Vitali et al., “Risks and Safety of CO2 Transport via Pipeline: A Review of Risk Analysis and Modeling Approaches for Accidental Releases”, Energies, vol. 14, 2021, 4601.
[9] L. Raimondi, “CCS Technology - CO2 Transportation and Relief Simulation in the Critical Region for HSE Assessment”, Chemical Engineering Transactions, vol. 91, 2022, pp. 43-48.
[10] S. T. McCoy and E. S. Rubin, “An engineering-economic model of pipeline transport of CO2 with application to carbon capture and storage”, International Journal of Greenhouse Gas Control, vol. 2, 2008, pp. 219-229.
[11] X. Luo, M. Wang, E. Oko, and C. Okezue, “Simulation-based Techno-economic Evaluation for Optimal Design of CO2 Transport Pipeline Network”, Applied Energy, vol. 132, 2014, pp. 610-620.
[12] V. E. Onyebuchi, A. Kolios, D. P. Hanak, C. Biliyok, and V. Manovic, “A systematic review of key challenges of CO2 transport via pipelines”, Renewable and Sustainable Energy Reviews, vol. 81, part 2, 2018, pp. 2563-2583.
[13] H. Lu, X. Ma, K. Huang, L. Fu, and M. Azimi, “Carbon dioxide transport via pipelines: A systematic review”, Journal of Cleaner Production, vol. 266, 2020, 121994.
[14] T. Clees et al., “MYNTS: Multi-phYsics NeTwork Simulator”, in Proc. of SIMULTECH 2016, International Conference on Simulation and Modeling Methodologies, Technologies and Applications, pp. 179-186, SciTePress, 2016.
[15] T. Clees, I. Nikitin, and L. Nikitina, “Making Network Solvers Globally Convergent”, Advances in Intelligent Systems and Computing, vol. 676, 2018, pp. 140-153.
[16] A. Baldin, T. Clees, B. Klaassen, I. Nikitin, and L. Nikitina, “Topological Reduction of Stationary Network Problems: Example of Gas Transport”, International Journal On Advances in Systems and Measurements, vol. 13, 2020, pp. 83-93.
[17] A. Baldin et al., “Principal component analysis in gas transport simulation”, in Proc. of SIMULTECH 2022, International Conference on Simulation and Modeling Methodologies, Technologies and Applications, pp. 178-185, SciTePress, 2022.
[18] A. Baldin et al., “On Advanced Modeling of Compressors and Weighted Mix Iteration for Simulation of Gas Transport Networks”, Lecture Notes in Networks and Systems, vol. 601, pp. 138-152, 2023.
[19] J. Nikuradse, “Laws of flow in rough pipes”, NACA Technical Memorandum 1292, Washington, 1950.
[20] P. Hofer, “Error evaluation in calculation of pipelines”, GWF-Gas/Erdgas, vol. 114, no. 3, 1973, pp. 113-119 (in German).
[21] J. Mischner, H. G. Fasold, and K. Kadner, System-planning basics of gas supply, Oldenbourg Industrieverlag GmbH, 2011 (in German).
[22] O. Kunz and W. Wagner, “The GERG-2008 wide-range equation of state for natural gases and other mixtures: An expansion of GERG-2004”, J. Chem. Eng. Data, vol. 57, 2012, pp. 3032-3091.
[23] W. Wagner, Description of the Software Package for the Calculation of Thermodynamic Properties from the GERG-2008 Wide-Range Equation of State for Natural Gases and Similar Mixtures, Ruhr-Universität Bochum, 2022.
[24] ISO 20765-2: Natural gas – Calculation of thermodynamic properties – Part 2: Single-phase properties (gas, liquid, and dense fluid) for extended ranges of application, International Organization for Standardization, 2015.

 ISBN: 978-1-68558-073-5